A Multiradius, Reciprocal Implementation of the Thin-Wire Moment Method

MARK A. TILSTON, MEMBER, IEEE, AND KEITH G. BALMAIN, FELLOW, IEEE

Abstract—**An implementation of the moment method for electromagnetic analysis of multiradius thin-wire structures, including multiwire, multiradius junctions is presented. It is entitled the multiradius bridge-current (MBC) moment method. It is an extension of the authors' uniradius bridge-current reformulation of Richmond's uniradius thin-wire theory. The method features an exactly symmetric mutual impedance matrix ensuring reciprocity between sources, it is unconstrained with respect to both the length ratio and the radius ratio of adjoining segments provided that the wires are electrically thin, and it permits the self-consistent inclusion of coaxial-cable sections in the configuration under analysis. The method is validated through comparison with transmission-line theory for a two-wire line and a coaxial cable, and through comparison with measurements on a sleeve monopole antenna and a log-periodic dipole antenna. Finally, the MBC moment method program is shown to surpass the Numerical Electromagnetics Code (NEC) in terms of reciprocity and convergence for both an AM broadcast tower detuning stub problem and a bent two-wire transmission-line problem.**

I. Introduction

A WELL-KNOWN moment method computer program for the electromagnetic analysis of uniradius thin-wire structures is that of Richmond [1]. It has been shown by Butler and Wilton [2] that the particular method of expansion and testing, which they term "Pocklington piecewise-sinusoid Galerkin," is one of the best methods for obtaining rapid convergence in the solution. Although very useful, Richmond's program can display asymmetric artifacts when used to analyze certain symmetric structures, a problem that was observed by Vainberg and Balmain [3], explained and corrected approximately by Hilbert, Tilston, and Balmain [4], and finally corrected more completely by the authors in their "bridge-current" formulation [5]. In the present work, the bridge-current formulation is extended to allow solution of the multiradius problem.

II. Description of Bridge-Current Moment Method Versions

A. Uniradius Bridge-Current Version

The uniradius bridge-current version forms the starting point for the multiradius bridge-current version. The uniradius version is described in detail in [5], and is described here briefly because it is necessary in order to explain the multiradius version.

The wire structure to be modeled consists of straight wire segments all of the same radius, and usually shorter than a quarter-wavelength. Conceptually, a current expansion function is a tubular dipolar current spanning the surface of two adjoining wire segments that are not necessarily collinear. Each expansion function has a corresponding indentical tubular testing function, in a coincident location. The current on each segment is axially directed, sinusoidally distributed, continuous at the segment junction, and zero at the other end of each segment. The total current at the junction is unity. The mutual impedance between a tubular expansion dipole and a tubular testing dipole is composed of four tubular-monopole-to-tubular-monopole mutual impedances.

The mutual impedance between a tubular expansion monopole and a tubular testing monopole is approximated by the mutual impedance between two filamentary monopoles that are placed on their respective segment axes unless the axes intersect or coincide. If the axes coincide, the expansion monopole is offset by a wire radius in a direction orthogonal to the coincident axes. If the two axes intersect, the expansion monopole is offset by a wire radius in a direction orthogonal to the plane containing both axes.

Now consider one testing monopole and two expansion monopoles that form an expansion dipole. With certain geometries, the filamentary expansion monopoles may be offset from their segment axes in different directions, thus forming a dipole that is broken at its vertex. This would occur, for example, if the segment axis of one, and only one, of the two expansion monopoles was coplanar with (but not parallel to) that of the testing monopole. In such a case, the break is bridged by a straight, uniformly distributed "bridge current." With this geometry, the bridge current is orthogonal to the testing monopole. Because of this orthogonality, and because of its uniform current distribution, the bridge current does not contribute to the following symmetric integral form for the mutual impedance Z_{ab} between a filamentary testing monopole a and a bridged filamentary expansion dipole b [5]:

$$Z_{ab} = j\omega \iint \left[\frac{\mu}{4\pi} \mathbf{J}_a(\mathbf{r}) \cdot \mathbf{J}_b(\mathbf{r}') + \frac{1}{4\pi\epsilon} \rho_a(\mathbf{r}) \rho_b(\mathbf{r}') \right] \frac{e^{-\gamma R}}{R} \, dV' \, dV \quad (1a)$$

where

$$R = |\mathbf{r} - \mathbf{r}'|, \quad (1b)$$

Manuscript received May 26, 1989; revised February 9, 1990. This work was supported by Bell Canada, by the Natural Sciences and Engineering Research Council, and by The Ontario Information Technology Research Centre.

M. A. Tilston was with the Department of Electrical Engineering, University of Toronto, Toronto, ON, Canada. He is now with M. A. Tilston Engineering, 90 Lawrence Avenue East, Toronto, ON, Canada M4N 1S6.

K. G. Balmain is with the Department of Electrical Engineering, University of Toronto, Toronto, ON, Canada M5S 1A4.

IEEE Log Number 9037639.

0018-926X/90/1000-1636$01.00

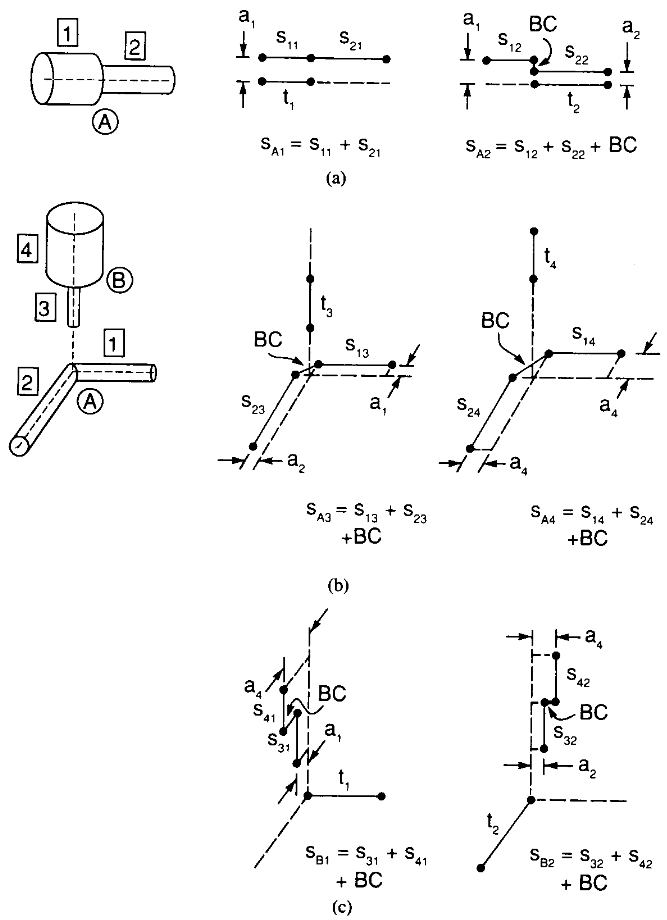

Fig. 1. Filamentary currents used to compute approximately (a) the self-impedance Z_{AA}, and (b) the mutual impedance Z_{AB}, of tubular dipoles. Circled letters and boxed numbers indicate tubular dipoles and monopoles. Dots denote endpoints of filamentary monopoles. t_j is a filamentary monopole having a longitudinal current distribution equal to tubular monopole j, and lying on the axis of j. s_{ij} is a filamentary monopole having longitudinal current distribution equal to tubular monopole i, but displaced from the axis of i in a manner that depends on tubular monopoles i and j. BC denotes bridge current, and a_i is the radius of monopole i. The point charge contribution of any monopole t_j is neglected.

and $\mathbf{J}$ and ρ are volume current and charge densities (unit terminal currents have been assumed). Thus the symmetric mutual impedance integral requires explicit computation of only the monopole-to-monopole mutual impedances which involve the monopole currents and the distributed charges. There are no point charges as the segment ends because current continuity is ensured due to the presence of the bridge current.

B. Multiradius Bridge-Current Version

Just as with the uniradius bridge-current version, the multiradius bridge-current version approximates the mutual impedance between tubular expansion and testing monopoles by using the mutual impedance between approximately equivalent filamentary expansion and testing monopoles. However, the amount of offset, if required, is modified to become the greater of the two segment radii. This offset is identical to the uniradius offset in the limiting case where the two segments are of equal radius. In addition, this offset scheme is valid in the limiting case where the radius of one segment is arbitrarily small and both axes are coincident (i.e., the segments are collinear). In this case the equivalence of mutual impedance between the pair of tubular monopoles and the pair of filamentary monopoles is exact because of symmetry. Examples showing the offsets involved in a dipole self-impedance and a dipole-to-dipole mutual impedance are given in Fig. 1.

Filamentary monopole-to-monopole mutual impedances are computed using (1a) without point changes. Apart from the inclusion of the monopole offsets as discussed above, the calculation of the inner products arising in (1a) is identical to the calculation described in [5] for the uniradius case. As with the uniradius version, a multiradius bridge current does not contribute to (1a) because of its orthogonality and uniform distribution.

With the above offsets and bridge currents, the mutual impedance between two filamentary monopoles does not depend on which one is the expansion monopole and which one is the testing monopole. The same must therefore be true of

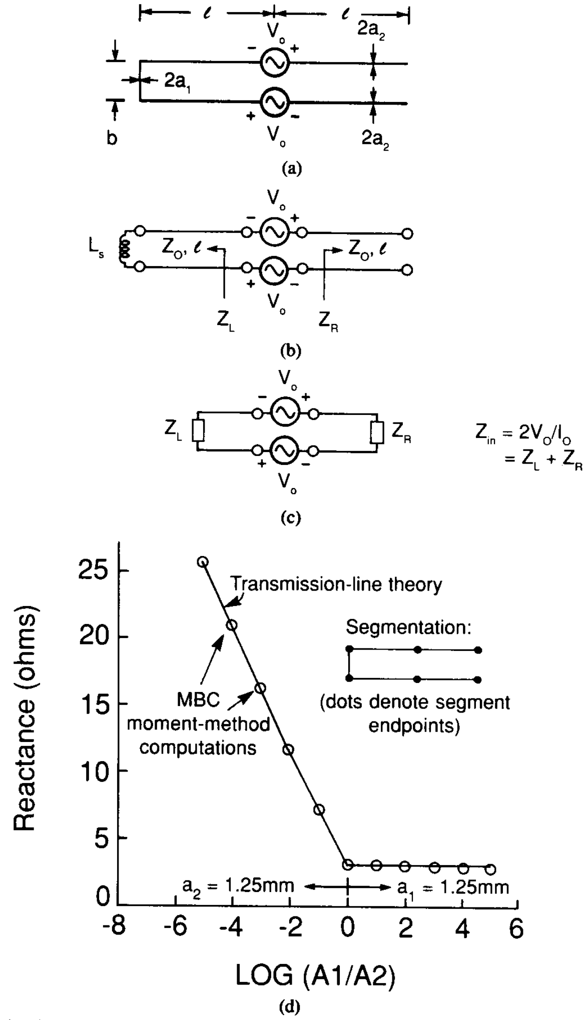

Fig. 2. Quarter-wave two-wire stub. (a) Feed points and dimensions. (b) Equivalent transmission line circuit. (c) Equivalent lumped element circuit. (d) Reactance for a frequency of 99.93 MHz and infinite conductivity. Transmission line theory (solid line) and MBC moment method computations (circles) are given for the segmentation shown.

filamentary dipoles. Thus, the dipole mutual impedance matrix is symmetrical. This is a necessary and sufficient condition for reciprocity to hold exactly between sources in the presence of any thin-wire structure that is modeled by the moment method.

III. Validation of Multiradius Bridge-Current Moment Method

Computations using the multiradius bridge-current (MBC) program will be compared with transmission-line theory for a resonant two-wire stub and a resonant coaxial cable stub, and compared with measurements for the sleeve monopole antenna and the log-periodic dipole antenna. Other structures that have been successfully analyzed by one of the authors [6] include the electrically small rectangular loop, the folded monopole antenna, and the bazooka-balun-fed dipole antenna.

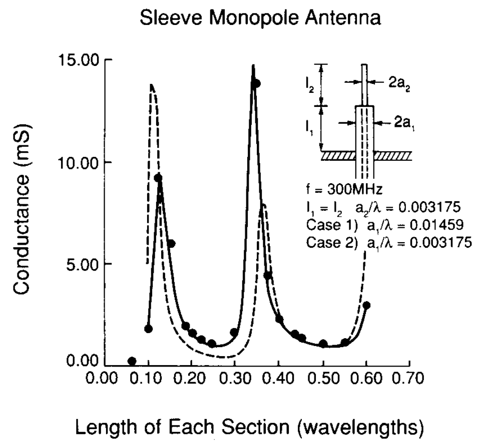

Fig. 3. Conductance versus length for sleeve monopole antenna. Dots and solid line denote measurements and MBC moment method computations respectively, for case 1. The dashed line denotes MBC moment method computations for case 2. In both cases, moment method computations include 15 segments in each of wires 1 and 2, and excitation by a frill source whose inner and outer radii are 0.003175 λ and 0.01459 λ.

The MBC moment method program was written in Fortran 77, and used double precision for all complex numbers and functions. The double precision was previously found to be necessary to obtain accurate input resistances for electrically small structures [5].

A. Resonant Two-Wire Quarter-Wave Stub

Transmission-line theory and the MBC moment method were used to compute the input reactance for the two-wire transmission line stub shown in Fig. 2(a) for varying wire radii as shown. The line has a width of 7.5 mm and a length of 750 mm, which is 0.25 λ at the test frequency of 99.93 MHz. The transmission line is short circuited at one end, and open circuited at the other.

Fig. 2(b) shows the equivalent transmission line circuit. The self-inductance L_S of the short-circuiting wire is approximately the same as the mutual inductance between two parallel filamentary currents spaced a wire radius apart.

The input reactance, as defined in Fig. 2(c), was computed with transmission-line theory and with the MBC moment method. The results are plotted in Fig. 2(d) for the transmission line with characteristic impedance varying between 212 and 1044 Ω. They show that good agreement was obtained, to within 0.2 Ω, despite the large difference in joined segments, with segment radius ratios of up to 10^5, and a longest-to-shortest segment length ratio of 50.

B. Sleeve Monopole Antenna

The sleeve monopole antenna consists of a coaxial cable that extends vertically up above a ground plane for some length, and has the outer conductor and dielectric filling removed over an upper portion of the length, as depicted in Fig. 3. The surface between the cut end of the outer conductor and the inner conductor is considered to be an aperture. The impedance is defined as the voltage from the outer conductor to the inner conductor at the aperture plane, di-

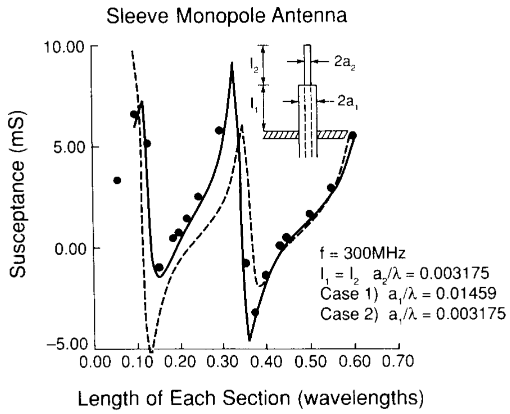

Fig. 4. Susceptance versus length for sleeve monopole antenna. Dots and solid line denote measurements and MBC moment method computations, respectively, for case 1. The dashed line denotes MBC moment method computations for case 2. In both cases, moment method computations include 15 segments in each of wires 1 and 2, and excitation by a frill source whose inner and outer radii are 0.003175 λ and 0.01459 λ.

vided by the current on the inner conductor at the aperture plane.

In the moment method analysis, the aperture is filled in with a perfect electric conductor, and an equivalent voltage source is introduced just above the aperture.

MBC moment method computations of the admittance of a sleeve monopole antenna have been compared with measurements by Taylor [7], for the geometry shown in Fig. 3. Initially, poor convergence in the moment method was observed, which was found to be due to the use of a delta source in combination with the relatively large electrical radius of the lower section of the antenna (0.015 λ).

A delta source is an infinitesimal source that produces a delta function of incident electric field along a testing monopole (whether tubular or filamentary) resulting in a single nonzero term in the moment method column matrix for voltage. A frill source is a finite-width magnetic current ring which is more realistic, as described in the Appendix. In order to compute the moment method excitation voltages, each tubular testing monopole is approximated by a filamentary monopole lying on the axis of the tube. This approximation greatly simplifies the computation of the reaction between the source and a testing current.

Good convergence with the frill source was observed when the lengths of the upper and lower sections on the antenna were each 0.15, 0.20, 0.35, and 0.45 wavelengths. The 0.45 wavelength case had the slowest convergence rate, requiring at least 15 segments on each antenna section. This number of segments was selected to be used for all the following computations.

Figs. 3 and 4 compare the computed and measured conductance and susceptance versus the length of each antenna section in wavelengths, shown as case 1. The conductance shows excellent agreement between computations and measurements, with the computed peaks appearing to coincide very well despite their sharpness. The susceptance curves are seen to agree well in shape but the computed values generally need to be shifted upward by 0.5 mS to agree with the measured ones. This shift is not a large amount, considering that it is equivalent to placing a 0.27 pF capacitor across the aperture.

The dashed lines in the figures are MBC moment method computations for case 2, which is similar to case 1, except that the radius of the lower half of the monopole is reduced to equal that of the top half. However, the frill source remains unchanged. This case is included to show that the radius change significantly affects the admittance curves.

It was noted that when the number of segments per antenna section was increased beyond a certain point, the solution diverged. This point corresponds approximately to a segment length-to-radius ratio of one. The divergence probably represents a failure in the filamentary current approximation for small segment-to-length ratios, as covered by Miller and Deadrick [8], and by Imbriale [9]. It might be overcome by using surface testing without approximation, as done by Imbriale [9] for a uniform dipole antenna.

C. Log-Periodic Dipole Antenna

Log-periodic dipole antenna (LPDA) analyses and measurements have been done by Vainberg and Balmain [3]. They investigated asymmetry resonances produced on LPDA's in which the symmetry was destroyed by the extension of one of the monopoles on the antennas. Their analysis used a uniradius computer model to approximate the multiradius physical antenna. This was done to enable them to utilize Richmond's (uniradius) thin wire moment method program [1]. It was noted that the program predicted significant asymmetry resonances even on a symmetric antenna model. This defect in the program was explained and corrected approximately in the paper by Hilbert, Tilston, and Balmain [4] on the subject of resonance phenomena of the LPDA. A more complete correction is given by Tilston and Balmain [5] in their uniradius bridge-current version of the program. In the present paper, computations with the MBC moment-method program are compared with measurements of the antenna side radiation for an asymmetrical antenna. This side radiation is due to unbalanced current in the two boom wires, and thus is a measure of the strength of the asymmetry resonance phenomenon.

The antenna has 14 monopole elements, labeled 1a, 1b, · · ·, 7a, 7b, as shown in Fig. 5(a). Also shown in the figure and caption are all wire dimensions. Monopole 5a is 2.9% longer than monopole 5b, in order to provide a physical asymmetry which will result in side-radiating resonances.

The antenna side radiation versus frequency is shown as the $\theta = 90°$ values in Fig. 5(b). The solid line shows results of the multiradius analysis, while the dashed line shows results of a uniradius analysis in which the boom diameter and spacing are scaled down by a factor of 2.01 so that the boom conductors are equal in radius to the monopole wires, while the characteristic impedance of the boom conductors remains unchanged. The uniradius results are essentially the same as those obtained by Vainberg and Balmain [3]. They show four well-defined resonant peaks that are similar to the measured values, except that they are shifted downward in

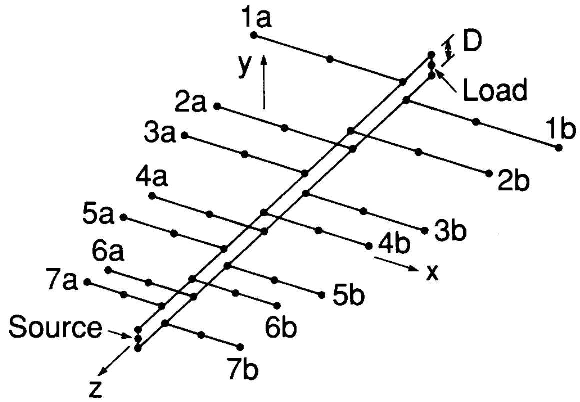

Monopole	Length (mm)	z (mm)
1a, 1b	137.4	-222.0
2a, 2b	122.4	-139.5
3a, 3b	109.1	-65.5
4a, 4b	97.0	0.0
5a	89.6	58.3
5b	87.1	58.3
6a, 6b	78.0	111.0
7a, 7b	69.8	157.0
source position:		194.5
load position:		-267.0

(a)

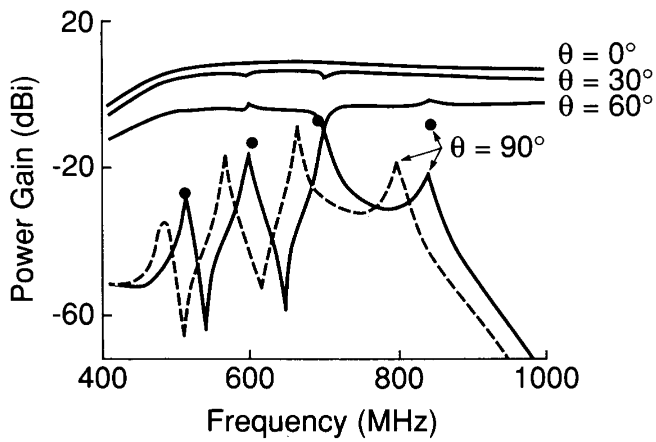

(b)

Fig. 5. Log periodic dipole antenna. (a) Segmentation and dimensions in computer model. Dots denote segment endpoints. Two cases of geometry are considered: a multiradius case in which all wires are 3.18 mm in diameter except for the z directed boom wires which are 6.40 mm in diameter, with $D = 14.6$ mm; and a single radius case in which all wires including the boom wires are 3.18 mm in diameter, with $D = 7.26$ mm. (b) E-plane theta-polarized gain versus frequency for the geometries in (a). Solid dots are measured values, and lines are computed with MBC moment method. Solid lines and solid dots are for the multiradius case. The dashed line is for the single radius case.

frequency by approximately 6%, or one third of the spacing between peaks. The multiradius results are seen to be in much better agreement with measured values in terms of resonant frequencies, with a shift in resonant frequency of 0.8% or less. The levels of the four resonant peaks are predicted to within 1, 2, 4, and 14 dB as frequency increases. This increasing error probably is due to the fact that, above 660 MHz (between the second and third resonances), the boom conductor radius exceeds the 0.007 λ upper limit originally specified by Richmond for thin-wire theory with a delta source as used in this computation.

D. Coaxial Cable Stub

Because the filamentary current distributions for testing and expansion currents in the MBC moment method are approximately equivalent to tubular surface distributions of testing and expansion currents, it should be possible to use filamentary currents to analyze structures containing thin concentric cylinders such as coaxial cables. To investigate this, an MBC moment method analysis of a coaxial cable stub was set up as follows for comparison with transmission line theory.

Consider the coaxial cable stub shown in Fig. 6(a). It has three tubular current-carrying surfaces consisting of the inner and outer surfaces of the outer conductor, and the single surface of the inner conductor. The frequency is 299.8 MHz, and the conductivity is 57 MS/m. Note that, in the moment method analysis, current is allowed to flow radially around the upper lip of the outer conductor, although not much would be expected. However, no radial current is allowed to flow on the bottom surface of the outer conductor, or the top surface of the inner conductor. All radial currents have zero divergence (i.e., no associated charge) because they are represented by uniform bridge currents in the filamentary current approximations.

The transmission-line theory included a series resistance per unit length using the same surface resistance R_s on the tubular metal surface as for a flat metal plate, i.e., the real

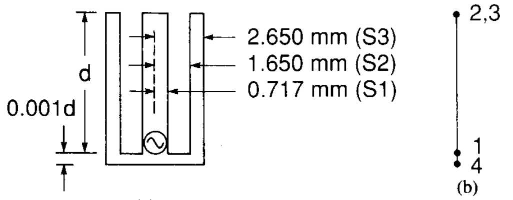

(a) (b)

Tubular Surface #	First Endpoint	Second Endpoint	Length	Radius (mm)
S1	1	2	d	0.717
S2	1	3	d	1.650
S3	3	4	1.01d	2.650

(c)

Note: Tubular surfaces with common endpoint numbers are electrically connected.

Fig. 6. Computational model of coaxial cable open-circuited stub. (a) Cross section showing dimensions. (b) Schematic showing axes of tubular surfaces as solid lines, and endpoints of the axes as dots and numbers. Each number represents a distinct electrical connection or a free end. (c) Specifications of tubular surfaces for program input.

part of the intrinsic impedance of the metal, which is

$$R_s \simeq \sqrt{\frac{\omega\mu}{2\sigma}} = 4.557 \times 10^{-3}\ \Omega.$$

The resistance per unit length of a cylindrical surface is the surface resistance divided by the circumference of the cylinder, which yields 1.012 Ω/m for the inner conductor and 0.440 Ω/m for the inner surface of the outer conductor. The sum of these two values is 1.452 Ω/m which is the total series resistance per unit length of the transmission line. The shunt conductance per unit length is zero. The series inductance and shunt capacitance per unit length of the line are 0.1668 μH/m and 66.71 pF/m. Under lossless conditions, these would yield a characteristic impedance of 50 Ω.

Computations of resistance and reactance for line lengths between 0.1 and 0.6 λ were done using the MBC moment method and transmission-line theory, as detailed by Tilston [6]. The MBC moment method model used three segments per tubular surface. MBC moment method computations generally agree with transmission-line theory to within 2% for both resistance and reactance (voltage reflection coefficients agree to within 5×10^{-5} in magnitude and 1.4° in phase).

It was noted that in the MBC results, current flowed radially over the upper lip of the outer conductor. The magnitude of this current was 17% of the generator current when the length was 0.25 λ.

An alternative moment method analysis was done in which the wall thickness of the outer conductor was reduced to zero. Thus, the outer conductor's outer and inner surfaces formed one single surface. This was modeled using only the first two of the three surfaces defined in Fig. 6(c). The MBC moment method computations using this model agreed as well with transmission-line theory as did the computations with the finite wall thickness.

The above comparisons were repeated for a short-circuited stub, and similarly good agreement was found.

Dielectric-filled coaxial cables have also been modeled using a procedure contained in Richmond's uniradius program for modeling a wire segment covered with a dielectric sheath [1]. The formulation involves replacing the dielectric with an equivalent electric current density $\mathbf{J}_d$ radiating in the ambient medium. Approximations are made that render $\mathbf{J}_d$ an easily computed quantity which is dependent on the local charge density on the wire. Thus no unknowns are added to the problem with the addition of the dielectric sheath.

The above coaxial stub examples were repeated, but representing RG-58 (dielectric filled) cable. The dielectric filling was treated as a dielectric sheath covering the inner conductor of the coaxial cable. The cable had radii of 0.538, 1.90, and 2.40 mm for three tubular surfaces. The conductor conductivity was 57 MS/m, and the dielectric had a relative permittivity of 2.3 and a loss tangent of 5×10^{-4}. For any line length between 0.1 and 0.6 wavelengths (in the dielectric), the voltage reflection coefficients computed by the MBC moment method and by transmission-line theory differed by a maximum of 5×10^{-4} in magnitude and 1.6° in phase for an open-circuited termination, and 5×10^{-4} in magnitude and 2.9° in phase for a short-circuited termination.

These moment-method computations with the dielectric required six segments per tubular surface for convergence, compared with three segments for the previous air-filled cable. In addition, although the accuracy for the dielectric-filled cable was lower, it would probably be acceptable for many applications.

IV. Comparison Between the MBC and NEC Programs

In this section, comparison between the multiradius bridge-current thin-wire moment method program and the Numerical Electromagnetics Code (NEC) [10] is given. The intent is not to make an extensive comparison, which would require coverage of a wide range of situations and many computations. Rather, the intent is simply to show that there are important cases in which the MBC moment method excels.

NEC is chosen for comparison because it is a well respected and widely used program. Version 1 is used here, but similar results have been obtained elsewhere using version 3 [11].

Two examples are selected for analysis. One involves a detuning stub used to minimize reradiation from a grounded tower near a monopole antenna in the AM broadcast band. The other involves a bent two-wire transmission line whose dimensions are typical of what one would find with conducting traces on a printed circuit board.

Because NEC uses single precision arithmetic and functions, a single-precision version of MBC is also used.

A. Tower Detuning Stub

Consider a simplified example of reradiation in the AM broadcast band, as depicted in Fig. 7(a). At the frequency of 1 MHz, the wavelength is approximately 300 m. Two towers

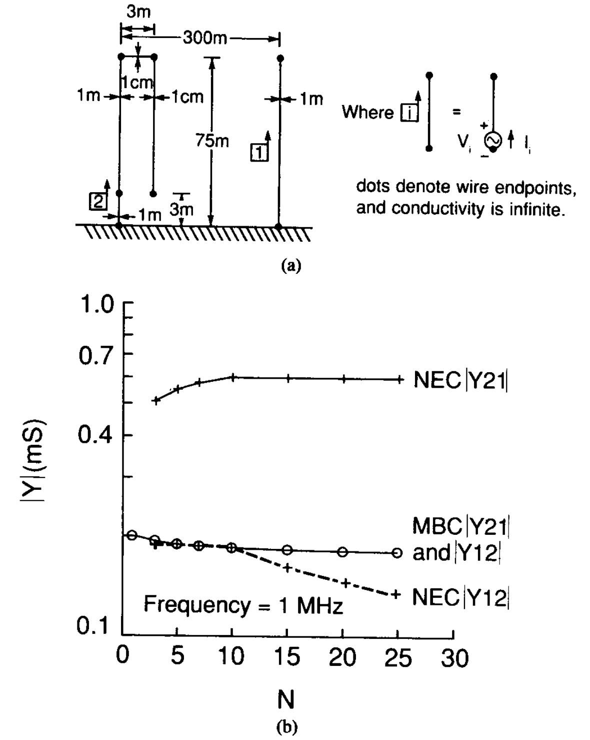

Fig. 7. Magnitude of mutual admittance between ports in detuning stub problem. (a) Geometry and port definitions. (b) Computations with MBC and NEC moment method programs. The two shortest wires have one segment each, while the remaining three wires have N segments each.

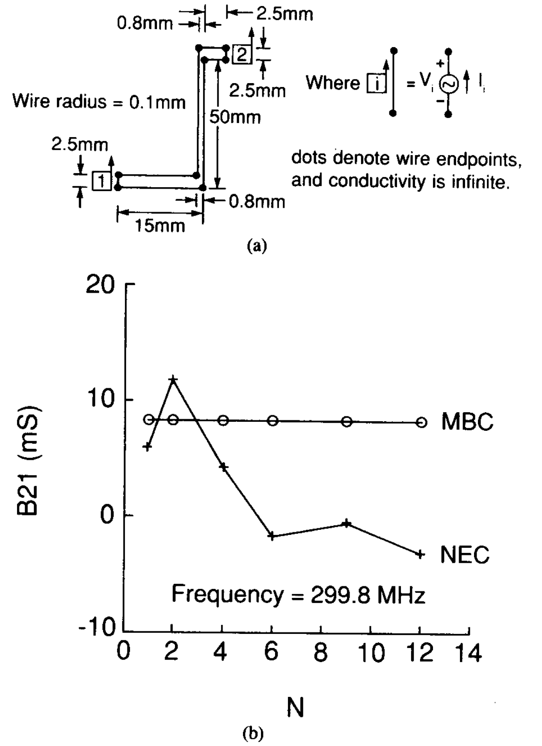

Fig. 8. Mutual susceptance between ports in bent two-wire transmission line. (a) Geometry and port definitions. (b) Computations with the MBC and NEC moment method programs. The four shortest wires have one segment each, while the remaining four wires have N segments each. Transmission line theory result is 8.61 mS.

75 m (0.25 λ) in height and 1 m in diameter are separated by 300 m (1 λ). The tower on the right represents a transmitting antenna. The one on the left represents some parasitic tower, which could be used to support an FM broadcast antenna for example. In order to reduce the amount of reradiation from the parasitic tower, a detuning stub has been added, consisting of wire 1 cm in diameter, and spaced 3 m from the tower axis. A common method of testing the effectiveness of the stub is to measure the base current of the parasitic tower (with a small loop antenna). This procedure is simulated on the computer, given a 1 V source at the base of the transmitting antenna. In other words, Y_{21} is computed. As a check on the numerical solution, the reciprocal quantity Y_{12} is also computed. Any difference between these two admittances indicates inaccuracy.

Computations of the mutual admittance magnitudes versus segmentation are shown in Fig. 7(b). A wide variation in results is seen. The MBC results show good convergence and exact reciprocity. With $N = 7$, the mutual admittance is 0.1877 mS with the stub, compared to 4.554 mS without the stub. This corresponds to a 28 dB reduction in base current due to the stub. The NEC results show significant nonreciprocity even though the Y_{21} appears well converged; however, Y_{12} begins to diverge for $N > 10$.

It should be mentioned that, in NEC, the "applied E-field" source was used. For comparison, the "current slope discontinuity" source was also tested. At a test segmentation of $N = 7$, the new NEC results were similar to the previous ones, except that the nonreciprocity error was somewhat worse. It was also found that the "extended thin wire kernel" option made no significant difference. This was probably due to the fact that the thickest wire was only 0.0033 λ in radius.

B. Bent Two-Wire Transmission Line

This example is a simplified representation of a small portion of a printed circuit board. One must be able to analyze this problem successfully, if one wishes to compute circuit board radiation or susceptibility. Fig. 8(a) represents two conducting traces on a printed circuit board that run from a pair of pins on one integrated circuit chip to a pair on another. The two wires, which represent traces, can carry a transmission line mode and a radiating mode. Only the transmission line mode is dealt with here: this is done by placing a shorting wire across each end of the transmission line. In the analysis, the four shortest wires, including the two short-circuiting wires, have one segment each, while each of the remaining four wires has a variable number of segments N. All wires are 0.1 mm in radius and the frequency is 299.8 MHz.

Computations of the mutual susceptance B_{21} versus segmentation are shown in Fig. 8(b). B_{12} was also computed, but is not shown because there was no significant nonreciprocity in either program. The MBC computations are seen to be extremely well converged, even when $N = 1$. As a check, B_{21} was also computed with transmission line theory, ignoring the effects of bends in the line and the inductance of the shorting wires. The result was 8.61 mS, which compares well with the value of 8.34 mS obtained by MBC for all N. It can be seen that the NEC results do not converge and are in poor agreement with transmission line theory.

V. Conclusion

The multiradius bridge-current moment method implementation presented herein has been validated through comparison with transmission-line theory and with experiments. The validation process involved the analysis of the following multiradius thin-wire structures: a resonant two-wire stub, a sleeve monopole antenna, a log-periodic dipole antenna, and a resonant coaxial cable stub. The latter case demonstrated the MBC moment method program's capability to model thin coaxial cables in a way that is both simple and self-consistent; moreover, it is shown that a dielectric-filled coaxial cable can be modeled very simply by utilizing an established representation for a dielectric sheath around a wire.

Some of the wire modeling quantities that the program has handled successfully in the above examples include a maximum wire radius ratio of 10^5 for joined wires, a maximum segment length ratio of 50 for joined segments, a maximum of three coaxial tubular conducting surfaces, a minimum segment length of 0.0025 λ, and a minimum segment length-to-radius ratio of one. These quantities are not necessarily limits of validity: they are merely examples that were studied. They show that the program allows the accurate and stable modeling of a very wide range of wire structures.

The multiradius analysis of the asymmetric log-periodic dipole antenna, including explicit modeling of the boom, has not previously been done, to the best of the authors' knowledge. The presented MBC moment method results agree well with measurements of the asymmetry-resonance frequencies and side-radiation levels. To obtain this agreement, it was necessary to use the physical boom dimensions for the wire radius and spacing, rather than the scaled-down dimensions that were previously used to permit a uniradius analysis. This establishes that the LPDA boom plays a crucially important part in the asymmetry resonance phenomenon. Moreover, this example shows that the LPDA provides a good general test case for a computational technique because it contains multiradius multiwire junctions, parallel wires carrying transmission-line modes, wires with free ends, and closed wire loops.

The MBC moment method is shown to perform better than NEC with respect to convergence and reciprocity for both an AM broadcast tower detuning stub problem, and a bent two-wire transmission-line problem.

Appendix

This Appendix derives the excitation voltage of a filamentary monopole of electric current due to a frill of surface magnetic current. Only the case in which the frill axis coincides with the monopole axis is covered here.

The excitation voltage V_j of a monopole j due to a general source of magnetic current $\mathbf{M}_g$ according to Richmond [12, eq. (12)] equals the following reaction between the monopole and the general source (assuming unit terminal currents):

$$V_j = -\int \mathbf{H}_i \cdot \mathbf{M}_g \, dv \tag{2a}$$

$$= \int \mathbf{E}_g \cdot \mathbf{J}_j \, dv. \tag{2b}$$

The second equation can be obtained from the first by applying the reciprocity theorem. For convenience, we will use the first equation.

Let the monopole be a linear electric current $\mathbf{I}_j$ on the z axis, flowing between points z_1 and z_2, and having unit feed-point current.

$$\mathbf{I}_j = \hat{\mathbf{z}} \frac{\sinh \gamma(z - z_l)}{\sinh \gamma(z_j - z_l)} \tag{3a}$$

$$= \hat{\mathbf{z}} \frac{1}{2 \sinh \gamma(z_j - z_l)} \sum_{p=1}^{2} m e^{-m\gamma z_l} e^{m\gamma z} \tag{3b}$$

where $j = 1$ or 2, $l = 2/j$, $m = (-1)^{p-1}$ and $z_1 \le z \le z_2$.

The magnetic vector potential $\mathbf{A}_j$ is

$$\mathbf{A}_j(\mathbf{r}) = \frac{\mu}{4\pi} \int_{z_1}^{z_2} \mathbf{I}_j(z') \frac{e^{-\gamma R}}{R} \, dz' \tag{4a}$$

$$= -\frac{\hat{\mathbf{z}}\mu}{8\pi \sinh \gamma(z_j - z_l)} \sum_{p=1}^{2} m e^{\gamma m(z - z_l)} \cdot \int_{u(z_1)}^{u(z_2)} \frac{e^{-u}}{u} \, du \tag{4b}$$

where $R = [\rho^2 + (z' - z)^2]^{1/2}$ and $u(z') = \gamma[R - m(z' - z)]$.

The magnetic field strength $\mathbf{H}_j$ is

$$\mathbf{H}_j = \frac{1}{\mu} \nabla \times \mathbf{A}_j = -\frac{\hat{\phi}}{\mu} \frac{\partial A_{jz}}{\partial \rho}. \tag{5}$$

Now consider a frill of magnetic surface current, centered at the origin, whose axis coincides with the z axis. The frill has inner radius a and outer radius b. The surface current $\mathbf{M}_f$ has the same distribution as the $\mathbf{E}$ field in a coaxial cable, as follows:

$$\mathbf{M}_f = \frac{-V_0}{\rho \ln b/a} \hat{\phi}, \qquad a \le \rho \le b, \quad z = 0. \tag{6}$$

Note that the total ϕ-directed magnetic current is $-V_0$ V. The $\mathbf{E}$ field of a frill is given by Butler and Tsai [13]. That would be required if we were using (2b). However, we will use (2a) instead, as follows:

$$V_j = -\int_a^b \int_0^{2\pi} \mathbf{H}_j \cdot \mathbf{M}_f \rho \, d\phi \, d\rho \tag{7a}$$

$$= -\frac{2\pi V_0}{\mu \ln(b/a)} \int_a^b \frac{\partial A_{jz}}{\partial \rho} \, d\rho \tag{7b}$$

$$= \frac{V_0}{4 \ln (b/a) \sinh \gamma (z_j - z_l)} \sum_{p=1}^{2} m e^{-\gamma m z_l} \cdot \sum_{h=1}^{2} (-1)^h \int_{u(z_1, \rho_h)}^{u(z_2, \rho_h)} \frac{e^{-u}}{u} \, du \tag{7c}$$

where $u(z', \rho) = \gamma([z'^2 + \rho^2]^{1/2} - mz')$, $\rho_1 = a$ and $\rho_2 = b$.

Note that the integration variable u is a complex constant multiplied by a real function. The integration path is therefore a straight line on the complex plane. The function

$$w_{12}(u_1, u_2) = \int_{u_1}^{u_2} \frac{e^{-u}}{u} \, du \tag{8}$$

for a straight line path is evaluated in Richmond's original program [1].

References

[1] J. H. Richmond, "Radiation and scattering by thin wire structures in a homogeneous conducting medium," *IEEE Trans. Antennas Propagat.*, vol. AP-22, p. 365, Mar. 1974. (Computer code available in: J. H. Richmond, "Computer program for thin wire structures in a homogeneous conducting medium," Nat. Tech. Inform. Service, Springfield, VA 22151, NASA CR-2399, June 1974.)

[2] C. M. Butler and D. R. Wilton, "Analysis of various numerical techniques applied to thin-wire scatterers," *IEEE Trans. Antennas Propagat.*, vol. AP-23, pp. 534-540, July 1975.

[3] M. Vainberg and K. G. Balmain, "On prediction of the asymmetry resonance phenomenon of log-periodic dipole antennas," *Can. Elec. Eng. J.*, vol. 6, no. 3, pp. 31-34, July 1981.

[4] M. Hilbert, M. A. Tilston, and K. G. Balmain, "Resonance phenomena of log-periodic antennas: Characteristic mode analysis," *IEEE Trans. Antennas Propagat.*, vol. AP-37, pp. 1224-1234, Oct. 1989.

[5] M. A. Tilston and K. G. Balmain, "On the suppression of asymmetric artifacts arising in an implementation of the thin-wire method of moments," *IEEE Trans. Antennas Propagat.*, vol. 38, pp. 281-285, Feb. 1990.

[6] M. A. Tilston, "Thin-wire reciprocal multiradius implementation of the electromagnetic moment method," Ph.D. dissertation, Dept. Elec. Eng., University of Toronto, Toronto, ON, Canada, 1989.

[7] J. Taylor, in *The Theory of Linear Antennas,* R. W. P. King. Cambridge, MA: Harvard Univ. Press, 1956, p. 416.

[8] E. K. Miller and F. J. Deadrick, "Some computational aspects of thin-wire modeling," in *Numerical and Asymptotic Techniques in Electromagnetics,* R. Mittra, Ed. New York: Springer-Verlag, 1975, pp. 112-114.

[9] W. A. Imbriale and P. G. Ingerson, "On numerical convergence of moment solutions of moderately thick wire antennas using sinusoidal basis functions," *IEEE Trans. Antennas Propagat.*, vol. AP-21, pp. 363-366, May 1973.

[10] G. J. Burke and A. J. Poggio, "Numerical electromagnetics code (NEC)—method of moments," Nat. Tech. Inform. Service, Springfield, VA 22151, NOSC TD 116, vol. 1 and 2, July 1977.

[11] G. A. Morin, personal communication.

[12] J. H. Richmond, "Radiation and scattering by thin-wire structures in the complex frequency domain," Nat. Tech. Inform. Service, Springfield, VA 22151, NASA CR-2396, May 1974.

[13] C. M. Butler and L. L. Tsai, "An alternate frill formulation," *IEEE Trans. Antennas Propagat.*, vol. AP-21, pp. 115-116, Jan. 1973.

Mark A. Tilston (M'79-S'82-M'82-S'82-M'86), for a photograph and biography please see page 1233 of the October 1989 issue of this Transactions.

Keith G. Balmain (S'56-M'63-SM'85-F'87), for a photograph and biography please see page 1234 of the October 1989 issue of this Transactions.